An Animal Model of Cutaneous Cyst Development Enables the Identification of Three Quantitative Trait Loci, Including the Homologue of a Human Locus (TRICY1)

Cosgarea, Ioana

2019-10

Cosgarea , I , Koelsch , B , Fischer , C , Griewank , K G , van den Berg , L , Kutritz , A , Schadendorf , D & Kindler-Röhrborn , A 2019 , ' An Animal Model of Cutaneous Cyst Development Enables the Identification of Three Quantitative Trait Loci, Including the Homologue of a Human Locus (TRICY1) ' , Journal of Investigative Dermatology , vol. 139 , no. 10 , pp. 2235-2238 . https://doi.org/10.1016/j.jid.2019.03.1154

http://hdl.handle.net/10138/314409
https://doi.org/10.1016/j.jid.2019.03.1154

Accepted Manuscript

An animal model of cutaneous cyst development enables the identification of three QTLs including the homologue of a human locus (*TRICY1*)

I. Cosgarea, B. Koelsch, C. Fischer, K.G. Griewank, L. van den Berg, A. Kutritz, D. Schadendorf, A. Kindler-Röhrborn

PII: S0022-202X(19)31495-2

DOI: https://doi.org/10.1016/j.jid.2019.03.1154

Reference: JID 1890

To appear in: *The Journal of Investigative Dermatology*

Received Date: 25 April 2018

Revised Date: 12 March 2019

Accepted Date: 13 March 2019

Please cite this article as: Cosgarea I, Koelsch B, Fischer C, Griewank KG, van den Berg L, Kutritz A, Schadendorf D, Kindler-Röhrborn A, An animal model of cutaneous cyst development enables the identification of three QTLs including the homologue of a human locus (*TRICY1*), *The Journal of Investigative Dermatology* (2019), doi: https://doi.org/10.1016/j.jid.2019.03.1154.

An animal model of cutaneous cyst development enables the identification of three QTLs including the homologue of a human locus (*TRICY1*)

I. Cosgarea[1,2#], B. Koelsch[3#], C. Fischer[4], K. G. Griewank[1], L. van den Berg[5], A. Kutritz[3], D. Schadendorf[1], A. Kindler-Röhrborn[3]

[1]Depatment of Dermatology, University Hospital of Essen, University of Duisburg-Essen, Essen, Germany.
[2]Dermatological Sciences, Institute of Cellular Medicine, Newcastle University, Newcastle upon Tyne, United Kingdom (Present address).
[3]Institute of Pathology, University Hospital of Essen, University of Duisburg-Essen, Essen, Germany.
[4]Institute of Human Genetics, University of Heidelberg, Heidelberg, Germany.
[5]Department of Biosciences (Genetics), Institute of Biotechnology, University of Helsinki, Helsinki, Finland.

[#]These authors have contributed equally to this work.

ORCiD Nr.:

I. Cosgarea – 0000-0002-2639-6264

B. Koelsch – 0000-0003-1031-9560

C. Fischer - 0000-0002-2144-5039

K. G. Griewank – 0000-0003-3899-9449

L. van den Berg – 0000-0001-5015-9106

A. Kutritz – 0000-0002-0517-7492

A. Kindler-Röhrborn – 0000-0002-2793-8854

Corresponding Author
Dr. Ioana Cosgarea
Dermatological Sciences, Institute of Cellular Medicine
Newcastle University
The Medical School
Framlington Place, NE2 4HH
Newcastle upon Tyne, United Kingdom
Email: ioana.cosgarea@newcastle.ac.uk

Short title: Three QTLs controlling cutaneous cyst formation in the rat

Abbreviations

BN - Brown Norway

chr. - chromosome

LE - Long Evans/Stm

LID - low iodine diet

MNU - N-methyl-N-nitrosourea

SNP - single-nucleotide polymorphismTPM -transcripts per million

Brief Summary

Using inbred BN and LE/Stm rats susceptible and resistant, respectively, to chemically induced cutaneous cyst development we were able to further unveil the genetic architecture of inherited multiple cyst formation. N-methyl-N-nitrosourea-treated (BN x LE) F_2 intercross rats proved to develop differential numbers of cutaneous cysts, demonstrating epidermal, trichilemmal and verrucous keratinization types. Male rats developed significantly more cysts per animal than females. QTL interval mapping yielded three loci on rat chromosomes 1, 8 and 11 (*Ccd1, Ccd2, Ccd3*) linked to cutaneous cyst formation. *Ccd2* proved to be homologous to the human *TRICY1* region which could further be narrowed down by genome comparison in both species. It contains 11 genes with evidence of expression in human keratinocytes.

To The Editor

Epidermal cysts represent benign skin tumors which can arise in any location, but more frequently on the scalp, face, upper back, neck and chest (Yang and Yang, 2009) due to traumatic inclusion of the epidermis in the dermis (Feng and Ma, 2015). While most patients develop individual cysts multiple lesions are seen in single cases (Yuksel and Tamer, 2016). Cases of hereditary trichilemmal cysts originating from the hair follicle have been reported in the literature (Seidenari et al., 2013). Leppard *et. al* demonstrated in 1977 that trichilemmal cysts can have an autosomal dominant mode of inheritance (Leppard et al., 1977).

Using inbred BN rats susceptible to chemically induced cutaneous cyst development and resistant LE/Stm rats (see supplemental data) we were able to establish a animal model for genetic dissection of multiple cyst formation.

282 low iodine diet (LID) treated (LE x BN) F2 intercross rats of both orientations received a single injection of the alkylating carcinogen N-methyl-N-nitrosourea (MNU), originally applied for inducing thyroid neoplasia, into the tail vein at 50 days of age (Supplementary Methods) as a study on the genetic architecture of sex-dependent thyroid cancer development was performed simultaneously. LID only treated BN rats had been shown not to develop cutaneous cysts. At 260 days animals were sacrificed followed by gross necropsy. The study was approved by the local administration's Ethical Committee on Experimental Animals (LANUV, Recklinghausen, Germany), in accordance with national legislation. Histologic examination revealed different types of cysts that developed in the lower dermis and subcutis with most cysts showing epidermal, or less frequently trichilemmal keratinization of the epithelium or mixtures of these keratinization types. In a few cases basophil granules in higher layers of the epithelium were reminiscent of a verrucous keratinization pattern (Figure 1A-F). Eighty-two (117/142) of male and 45% (63/140) of female rats presented cutaneous cysts. Additionally male rats tend to develop more cutaneous cysts/animal than female rats

(Figure 1G; Supplementary Table S1A). The parental orientation of crosses (LE x BN) vs. (BN x LE) did not influence the development of cutaneous cysts (p = 0.28; Supplementary Table S1B).

Because in contrast to highly susceptible BN males all BN females and the majority of female F_2 rats did not develop cutaneous cysts QTL interval mapping analysis was performed with 106 SNPs (average marker density 30 Mb) using DNAs from 142 male F_2 hybrids of both orientations (Supplementary Methods). Three QTLs linked to cyst numbers residing on chromosomes 1, 8 and 11 (*Ccd1*, *Ccd2* and *Ccd3)* proved to surpass the genome wide significance threshold (LOD score 3,74; see Fig. 1 H).

Figures 2 A-C visualize the strongest linkage between cutaneous cyst numbers/F_2 male and genotype recorded for SNPs on chromosomes 1, 8 and 11. While F_2 males with homozygous BN alleles for the SNP 213.36 Mb on chr.1 located in the *Ccd1* locus and the SNP at 125.88 Mb in *Ccd2* on chr.8 display comparatively high numbers of cysts/animal, heterozygous males show less cysts and male F_2 rats carrying homozygous LE alleles present the lowest numbers cyst/animal (Figures 2A and B) suggesting an allele dose effect.

For the SNP 76.11 Mb in *Ccd3* on chr.11, the situation is reverse as homozygous LE alleles are associated with a higher number of cutaneous cysts, while heterozygous and homozygous BN alleles seem to mediate equally low numbers of cutaneous cysts (Figure 2C). Other studies have also indicated that in segregating crosses animals with a tumor resistance phenotype can transmit susceptibility alleles that in the resistant animals are obviously counteracted by opposing factors (Fijneman et al., 1996, Koelsch et al., 2006).

Multiple QTL analysis taking the three genome wide significant loci into consideration revealed a model with three main effects y ~ Q1 + Q2 + Q3. Stepwise regression analysis revealed that no further QTLs nor two way interaction terms met the significance criteria for inclusion in the model; for description of locus interaction see suppl. Figs. 1A-C. The three

loci explain a large portion of 40% of phenotypic variance. Still multiple other loci may influence through weaker effects as well as random effects cyst numbers, too. The further could not be identified due to power restrictions.

Interestingly, the *Ccd2* locus on rat chr.8 is perfectly homologous to the human *TRICY1* locus on chromosome 3 associated with the hereditary occurrence of trichilemmal cysts within a Danish family (Eiberg et al., 2005), see Figure 2D. Eiberg *et al.* further excluded coding mutations in the *CTNNB1 and MLH1* genes, reported to be involved in inherited hair defects, via sequencing (Eiberg et al., 2005). The region of interest of the rat locus could be shortened by approximately 5 Mb not present in the core region of human *TRICY1* which consists of two neighboring gene blocks displaying 43 and 26 genes, respectively. In the rat genome these blocks are separated by a sequence fragment also absent in the core region of *TRICY*, the block on the 5' end being inverted compared with *TRICY*.

The analysis of 14 male cysts carrying F_2 rats recombinant between flanking SNP markers at 111.85 Mb and 125.88 Mb on rat chromosome 8 revealed that the resistance genotype (LE/LE) is present in 13/14 animals at proximal SNP (111.85 Mb) but only in one animal at *Acaa1a* (124.3 Mb) and the distal SNP (125.88 Mb), Therefore the susceptibility gene is likely to reside in the gene block flanked by *Golga4* and *Ctnnb1* between 123,1 Mb and 126 Mb supported by the highest LOD score at 125 Mb (see Figure 2D and Supplemental Figure 3). According to the human protein atlas (http://www.proteinatlas.org) 22 of the 40 genes located in the candidate region encode proteins that are expressed in the human skin and among them 11 genes, *ZCWPW2, CMC1, GOLGA4, ITGA9, OXSR1, MYD88, GORASP1, SLC25A38, RPSA, RPL14* and C*TNNB1* are expressed in keratinocytes. Expression was quantified by RNA-seq in TMP values for humans as indicated in Supplemental Table 2.

According to the rat genome data base Golga4 and Myd88 carry amino acid changing polymorphisms between the BN reference genome and the genomic sequence of LE/Stm (https://rgd.mcw.edu/jbrowse).

In summary we identified three loci associated with cutaneous cyst formation (*Ccd1, Ccd2,* and *Ccd3*) located on chromosomes 1, 8 and 11 with genome wide significance applying a genetic rat model, to our knowledge previously unreported. *Ccd2* is homologous to the human *TRICY1* region which could further be narrowed down by genome comparison in both species. Future studies of this model and correlations with human data are likely to identify the genes predisposing to and involved in cutaneous cyst formation.

Data availability statement

Datasets related to this article can be found at https://data.mendeley.com/datasets/gp9k5y2y7k/1, hosted at Mendeley (http://dx.doi.org/10.17632/gp9k5y2y7k.1#file-725d5fdc-f13e-4d3f-a8ec-4059e1d98802).

Conflict of Interest

The authors state no conflict of interest.

Acknowledgements

This study was funded by the Federal Ministry of Research and Technology (BMBF); Grant number 01FP1062/63. The authors thank Armin Daschke, and Marcus Linnenboden, Central Animal Facility, University Hospital of Essen, University of Duisburg-Essen, Essen, Germany for expert assistance with animal husbandry.

I. Cosgarea[1,2#], B. Koelsch[3#], C. Fischer[4], K. G. Griewank[1], L. van den Berg[5], A. Kutritz[3], D. Schadendorf[1], A. Kindler-Röhrborn[3]

CRediT statement

Author contributions for the present manuscript:

1. Conceptualization: A. Kindler-Röhrborn, B. Koelsch
2. Data curation: B. Koelsch, I. Cosgarea
3. Formal analysis: C. Fischer
4. Funding acquisition: A. Kindler-Röhrborn
5. Investigation: I. Cosgarea, B. Koelsch, K. Griewank, L. van den Berg, A. Kutritz, A. Kindler-Röhrborn
6. Methodology: I. Cosgarea, B. Koelsch, A. Kindler-Röhrborn
7. Project administration: A. Kindler-Röhrborn
8. Resources: A. Kindler-Röhrborn, B. Koelsch
9. Software: C. Fischer
10. Supervision: A. Kindler-Röhrborn
11. Validation: B. Koelsch
12. Visualization: I. Cosgarea, B. Koelsch, K. Griewank, L. van den Berg, D. Schadendorf, C. Fischer, A. Kindler-Röhrborn
13. Writing – original draft: I. Cosgarea, B. Koelsch, C. Fischer, A. Kindler-Röhrborn
14. Writing – review& editing: I. Cosgarea, B. Koelsch, C. Fischer, A. Kindler-Röhrborn

References

Eiberg H, Hansen L, Hansen C, Mohr J, Teglbjaerg PS, Kjaer KW. Mapping of hereditary trichilemmal cyst (TRICY1) to chromosome 3p24-p21.2 and exclusion of beta-CATENIN and MLH1. Am J Med Genet A 2005;133A(1):44-7.

Feng CJ, Ma H. Treatment of epidermal cysts with erbium: YAG laser fenestration: an alternative to surgical intervention. Ann Plast Surg 2015;74 Suppl 2:S89-92.

Fijneman RJ, de Vries SS, Jansen RC, Demant P. Complex interactions of new quantitative trait loci, Sluc1, Sluc2, Sluc3, and Sluc4, that influence the susceptibility to lung cancer in the mouse. Nat Genet 1996;14(4):465-7.

Koelsch BU, Fischer C, Neibecker M, Schmitt N, Schmidt O, Rajewsky MF, et al. Gender-specific polygenic control of ethylnitrosourea-induced oncogenesis in the rat peripheral nervous system. Int J Cancer 2006;118(1):108-14.

Leppard BJ, Sanderson KV, Wells RS. Hereditary trichilemmal cysts. Hereditary pilar cysts. Clin Exp Dermatol 1977;2(1):23-32.

Seidenari S, Pellacani G, Nasti S, Tomasi A, Pastorino L, Ghiorzo P, et al. Hereditary trichilemmal cysts: a proposal for the assessment of diagnostic clinical criteria. Clin Genet 2013;84(1):65-9.

Yang HJ, Yang KC. A new method for facial epidermoid cyst removal with minimal incision. J Eur Acad Dermatol Venereol 2009;23(8):887-90.

Yuksel ME, Tamer F. Multiple widespread epidermal cysts of the skin: an unusual presentation. Acta Dermatovenerol Alp Pannonica Adriat 2016;25(2):23-4.

Figure Legends

Figure 1. Cutaneous cysts: Histology, sex difference and QTL mapping. a and d. Cysts with epidermal keratinization of the epithelium. **b and e**. more trichilemmal differentiation. **c and f**. occasionally observed verrucous keratinization pattern. Magnifications 20x or 200x as indicated. **g.** Distributions of cutaneous cysts/animal for male and female (LE x BN) F_2 rats depicted as dot plots. **h**. QTL interval mapping of cyst multiplicity. The solid horizontal line represents the genome wide significance level of 5% (lod score 3,74) as calculated by permutation analysis. Scale bar = 1 mm in a, b, c. Scale bar = 200 μm in d, e, f.

Figure 2. Gene loci linked to cyst multiplicity. a-c Distributions of cyst numbers/animal depending on genotypes for SNPs on chromosome 1, 8 and 11 linked to cyst multiplicity displayed as dot plots. Panel A: SNP on chromosome 1, at 213.36 Mb. B: SNP on chromosome 8 at 125.88 Mb. C: SNP on chromosome 11 at 76.11 Mb. **b. Alignment of human and rat *TRICY1/Tricy1* loci**. Upper part shows the human region on chromosome 3 representing the *TRICY1* locus (yellow) flanked by markers D3S3559 and D3S2432; numbers of human genes as indicated by UCSC map (hg38). Lower part presents the complete rat *Ccd2* locus between SNPs at 112 Mb and 126 Mb (red) and homologous regions between the rat and human loci (red and yellow) according to the UCSC rat 2004 map. Blue and green genomic segments are not included in the human locus but flanking it. The sequence of the *Ccd2* locus is interrupted by the blue colored fragment and consists in both species of two conserved gene blocks from *Mlh1* to *Gpd1l* and *Golga4* to *Ctnnb1*, the latter one inverted in the rat. Segment ends: Mb position on the corresponding chromosomes. Red arrows: breakpoints between human and rat gene order. Lines between chromosomes: interspecies chromosome segmental shift and orientation.

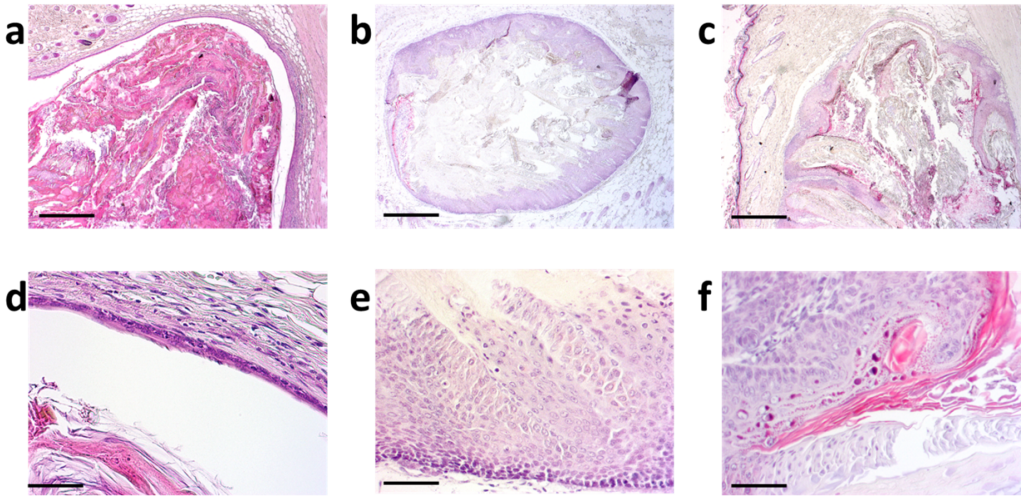
a
b
c
d
e
f

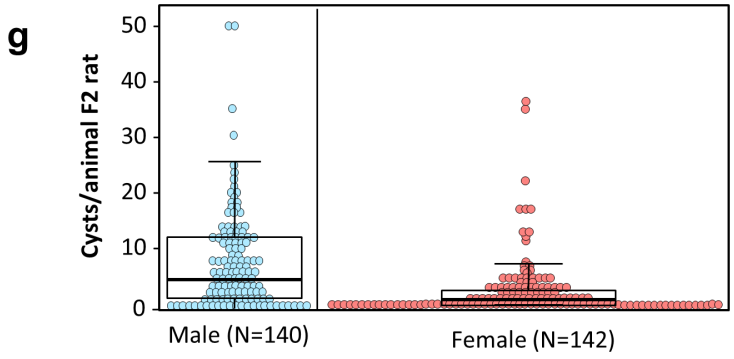
g
Cysts/animal F2 rat
50
40
30
20
10
0
Male (N=140)
Female (N=142)

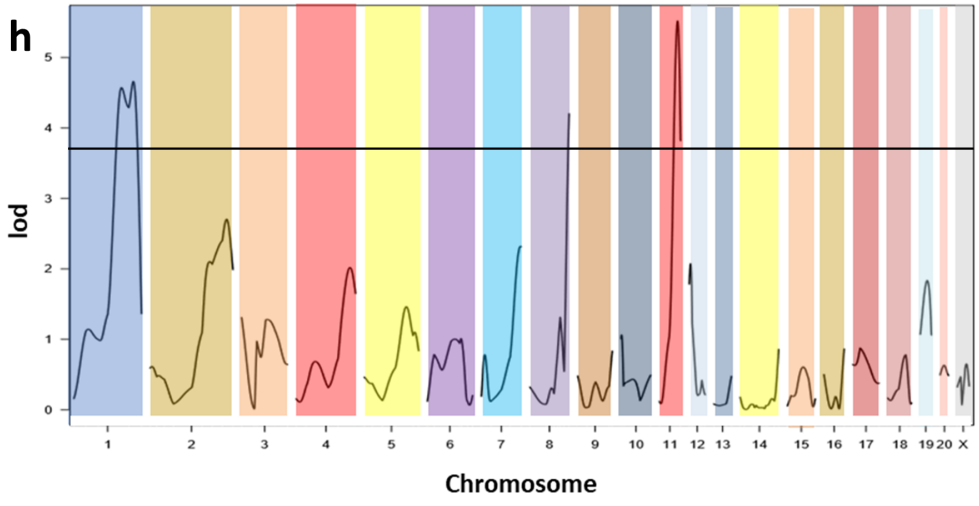
h
lod
5
4
3
2
1
0
1
2
3
4
5
6
7
8
9
10
11
12
13
14
15
16
17
18
19
20
X
Chromosome

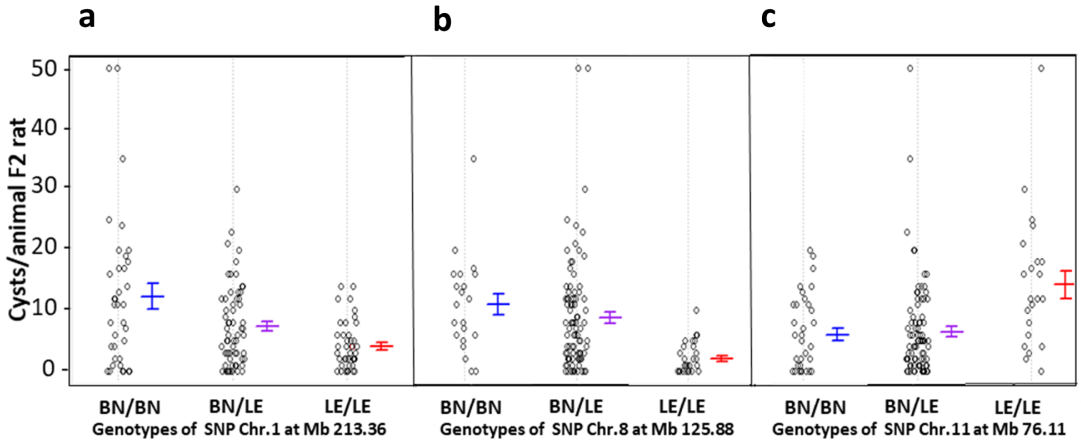
a
b
c
Cysts/animal F2 rat
50
40
30
20
10
0
BN/BN
BN/LE
LE/LE
Genotypes of SNP Chr.1 at Mb 213.36
Genotypes of SNP Chr.8 at Mb 125.88
Genotypes of SNP Chr.11 at Mb 76.11

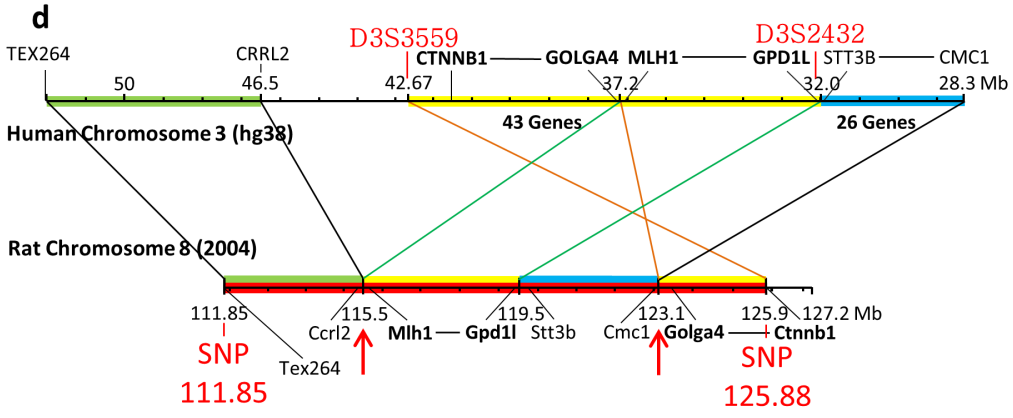
d
TEX264
CRRL2
D3S3559
CTNNB1
GOLGA4
MLH1
D3S2432
GPD1L
STT3B
CMC1
50
46.5
42.67
37.2
32.0
28.3 Mb
43 Genes
26 Genes
Human Chromosome 3 (hg38)
Rat Chromosome 8 (2004)
111.85
115.5
119.5
123.1
125.9
127.2 Mb
SNP
111.85
Tex264
Ccrl2
Mlh1
Gpd1l
Stt3b
Cmc1
Golga4
Ctnnb1
SNP
125.88

Suplementary Material

Supplementary Methods

Induction of cutaneous cysts

Carcinogen

N-methyl-N-nitrosourea (MNU) was purchased from Sigma-Aldrich (Munich, Germany; purchase number N4766-25), stored at 4°C and dissolved immediately before use in 0.2 M Na2HPO4/0.1 M citrate buffer (pH 6.0) at 10mg/ml.

Experimental design

As a study on the genetics of sex-dependent thyroid cancer was performed simultaneously, (LE x BN) F_2 intercross rats of both orientations and sexes were fed a low iodine diet (C1042; Altromin Spezialfutter GmbH, Lage, Germany) after weaning at 28 days of age. At 50 days of age they received a single injection of MNU (40 mg/kg body weight) into the tail vein. All rats were sacrificed at 260 days and gross necropsy was performed. Skin tumors were identified visually and through careful palpation examination of the animals' fur. Pathologically altered tissue was fixed in formalin and embedded in paraffin for histological analysis

DNA isolation and genotyping

DNA was isolated from (LE x BN) F2 rat tail biopsies taken at day 28 and genotyped by LGC Genomics Ltd. / KBIO science (Hoddesdon /Herts, UK) using 106 genome-wide distributed SNP markers. The location of markers is based on the 2004 version of the rat genome.

Statistical analysis

First we performed a standard single QTL interval mapping analysis using maximum likelihood estimation via the EM algorithm with the software R/QTL by Broman using a high resolution genetic map (Bromann and Sen, 2009, Littrell *et al.*, 2018). Genome wide significance level was calculated by a permutation approach with 1000 permutation replicates. Secondly, in a multiple- QTL analysis we fit the genomewide significant loci from the first step coding each locus as an additive effect and dominance deviation. We then explored this model for the possibility of further QTLs and two way interactions. As recommended by Broman for a systematic search we used the Haley-Knott regression frame work. We performed forward selection to a model with 5 QTL, followed by backward elimination, and reported the model giving the largest penalized LOD score.

As a sensitivity analysis for the standard single QTL interval mapping we additionally performed nonparametric QTL interval mapping.

References:

Bromann, K. and S. Sen (2009) A Guide to QTL Mapping with R/qtl, Springer.

Littrell, J., S. W. Tsaih, A. Baud, P. Rastas, L. Solberg-Woods and M. J. Flister (2018) A High-Resolution Genetic Map for the Laboratory Rat. *G3 (Bethesda)* 8(7): 2241-2248.

Supplementary data:

In a previous study cutaneous cysts were recorded in 39 BN - and 38 LE/Stm rats previously treated with MNU and IDD during an observation period of 260 days. While neither LE rats of both sexes nor female BN rats developed cutaneous cysts 16/17 (94 %) of BN males developed numerous cysts leading to a premature termination of the experiment in a number of animals at the discretion of the animal facility's veterinarian service. Therefore comparative quantification of cysts was not possible.

rat strain	N	Cases with epidermal cysts
BN males	17	16
BN females	21	0
LE males	20	0
LE females	21	0

Supplemetary TableS1

Table S 1A

Comparison of cyst numbers of 282 (LE x BN) F_2 intercross rats by sex and orientation							
		mean, CI[1]	**median**	**Q 25[2]**	**Q 75[3]**	**IQR[4]**	**p-values**
males		7.61 6.19 – 9.02	5.0	3	13	10	< 0.0001
females		2.67 1.74-3.60	1.0	0	3	3	
all animals	(LE x BN)	5.27 3.86-6.68	2.0	0	7	7	0.28
	(BN x LE)	5.03 3.95–6.11	3.0	0	8	8	

Table S 1B

Comparison of cyst numbers in male and female (LE x BN) F_2 intercross rats by cross orientation							
		mean, CI[1]	**median**	**Q25[2]**	**75Q[3]**	**IQR[4]**	**p- value**
males	(LE x BN)	7.05 4.33-9.28	4.0	1	9	8	0.048
	(BN x LE)	8.22 6.49-9.96	6.0	3	12	9	
females	(LE x BN)	3.44 1.78-5.10	0.0	0	3.5	3.5	0.854
	(BN x LE)	1.84 1.10-2.57	1.0	0	3	3	

[1] confidence interval, [2]quartile 25, [3]quartile 75, [4] interquartile range

Table S2

Genes annotated in the rat chromosome-8 candidate region

Position on rat chromosom 8 rn6 (2014)				GTEx RNA-seq expression values in TPM* in human skin		
Start#	Stop#	Gene symbol	Description			
124310288	124399345	Tgfbr2	transforming growth factor, beta receptor II	58		
124833537	125544624	Rbms3	RNA binding motif, single stranded interacting protein 3	4		
126268760	126402046	Zcwpw2	zinc finger CW-type and PWWP domain containing 2	1		
126411044	126435581	Azi2	5-azacytidine induced 2	14		
126437345	126495347	Cmc1	C-x(9)-C motif containing 1	5		
127065292	127726248	Ctdspl	CTD small phosphatase like	44		
127144368	127152618	Eomes	eomesodermin	0		
127171326	127248938	Golga4	golgin A4	39	Candidate gene most likely location	Overlap of rat candidate region with human 43 gene block (see figure 2D)
127270929	127576709	Itga9	integrin subunit alpha 9	3		
127714441	127714530	Mir26a	microRNA 26a	0		
127735233	127753313	Vill	villin-like	12		
127753514	127782070	Plcd1	phospholipase C, delta 1	32		
127789011	127835905	Dlec1	deleted in lung and esophageal cancer 1	1		
127836237	127845028	Acaa1b	acetyl-Coenzyme A acyltransferase 1B	no data		
127858425	127871192	Slc22a14	solute carrier family 22, member 14	0		
127885268	127900469	Slc22a13	solute carrier family 22 member 13	0		
127920349	128009951	Oxsr1	oxidative-stress responsive 1	29		
128022512	128027461	Myd88	myeloid differentiation primary response 88	32		
128027880	128036471	Acaa1a	acetyl-CoA acyltransferase 1 (human ACAA1)	333		
128041677	128076951	Xylb	xylulose kinase	1		
128087315	128118844	Acvr2b	activin A receptor type 2B	1		
128133405	128153110	Exog	exo/endonuclease G	2		
128169191	128266639	Scn5a	sodium voltage-gated channel alpha subunit 5	no data		
128298593	128416897	Scn10a	sodium voltage-gated channel alpha subunit 10	0		
128450793	128521129	Scn11a	sodium voltage-gated channel alpha subunit 11	0		
128577080	128610287	Wdr48	WD repeat domain 48	15		
128610290	128622337	Gorasp1	golgi reassembly stacking protein 1	27		
128622403	128657199	Ttc21a	tetratricopeptide repeat domain 21A	2		
128659883	128673335	Csrnp1	cysteine and serine rich nuclear protein 1	81		
128702180	128712075	Xirp1	xin actin-binding repeat containing 1	0		
128738689	128755376	Cx3cr1	C-X3-C motif chemokine receptor 1	0		
128781208	128782531	Ccr8	C-C motif chemokine receptor 8	0		
128790348	128802988	Slc25a38	solute carrier family 25, member 38	29		
128806056	128809987	Rpsa	ribosomal protein SA	1019		
128824408	128854492	Mobp	myelin-associated oligodendrocyte basic protein	0		
128972383	129139257	Myrip	myosin VIIA and Rab interacting protein	1		
129158112	129160726	Eif1b	eukaryotic translation initiation factor 1B	78		
129201000	129232436	Entpd3	ectonucleoside triphosphate diphosphohydrolase 3	3		
129240528	129243400	Rpl14	ribosomal protein L14	1268		
129617770	129628378	Ctnnb1	catenin beta 1	107		

*** TPM (transcripts per million) median values from https://gtexportal.org/home/**
Protein to transcript level correlation is often weak

 # Note that SNP and gene positions in the main text refer to rat genome version rn4 (Map 2004)

Figures S1a – c. Two dimensional effect plots of all combinations of two of the genome wide significant QTLs found in the single QTL analysis. Distributions of cyst numbers/F_2 animal depending on combinations of genotypes for SNPs at Chr.8 at 125,88 Mb, at Chr.1 at 213,36 Mb and atChr.11 at 76,11 Mb.

a

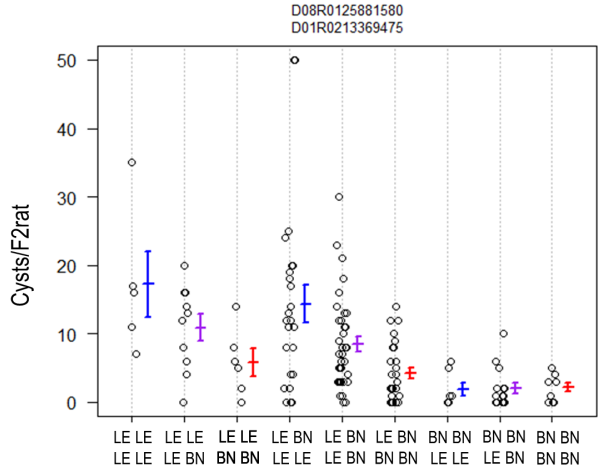
D08R0125881580
D01R0213369475
Cysts/F2rat
0
10
20
30
40
50
LE LE LE LE
LE LE LE BN
LE LE BN BN
LE BN LE LE
LE BN LE BN
LE BN BN BN
BN BN LE LE
BN BN LE BN
BN BN BN BN

b

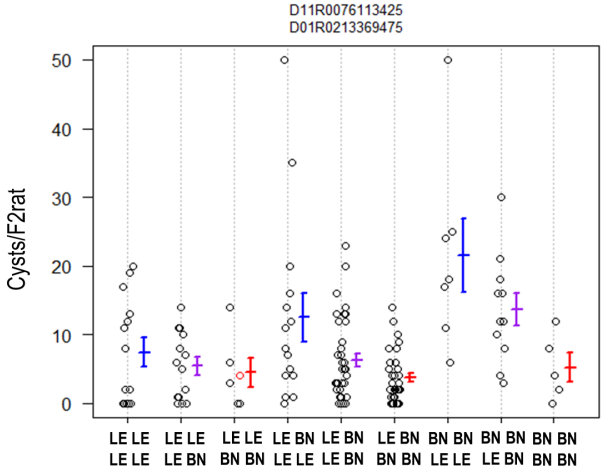
D11R0076113425
D01R0213369475
Cysts/F2rat
0
10
20
30
40
50
LE LE LE LE
LE LE LE BN
LE LE BN BN
LE BN LE LE
LE BN LE BN
LE BN BN BN
BN BN LE LE
BN BN LE BN
BN BN BN BN

c

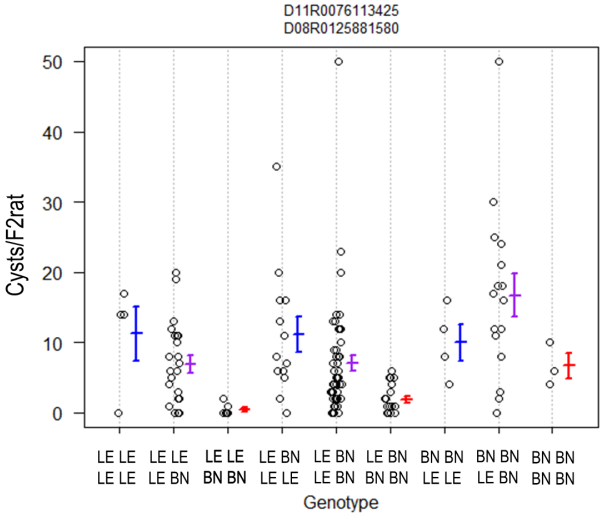
D11R0076113425
D08R0125881580
Cysts/F2rat
0
10
20
30
40
50
LE LE LE LE
LE LE LE BN
LE LE BN BN
LE BN LE LE
LE BN LE BN
LE BN BN BN
BN BN LE LE
BN BN LE BN
BN BN BN BN
Genotype

Supplementary Figure S2

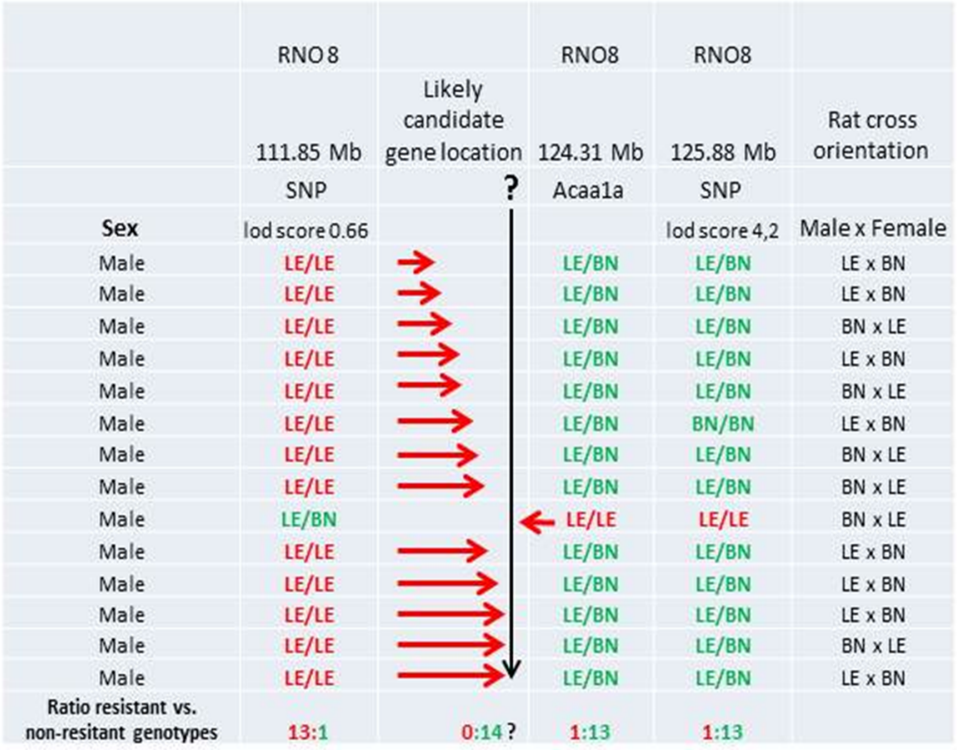

Figure S2. **Genotypes of 14 cyst carrying male F2 rats recombinant between SNPs at 111.85 and 125.88 Mb on rat chromosome 8 with additional genotypes of a SNP at 124.31.** Resistance genotypes are depicted in red and susceptible genotypes in green. Central vertical line in black shows the likely position of the gene/regulatory element underlying cyst susceptibility close to Acaa1a. However the trait is not monogenic; therefore cyst bearing rats may display LE/LE resistance alleles with incomplete penetrance at the chr. 8 candidate locus. Column3 from the left shows fictitious statistical distribution of alternative breakpoints (red arrow heads).

Figure S2. **Genotypes of 14 cyst carrying male F2 rats recombinant between SNPs at 111.85 and 125.88 Mb on rat chromosome 8 with additional genotypes of a SNP at 124.31.** Resistance genotypes are depicted in red and susceptible genotypes in green. Central vertical line in black shows the likely position of the gene/regulatory element underlying cyst susceptibility close to Acaa1a. However the trait is not monogenic; therefore cyst bearing rats may display LE/LE resistance alleles with incomplete penetrance at the chr. 8 candidate locus. Column3 from the left shows fictitious statistical distribution of alternative breakpoints (red arrow heads).